Removal of chromium from synthetic wastewater using MFI zeolite membrane supported on inexpensive tubular ceramic substrate

R. Vinoth Kumar and G. Pugazhenthi

ABSTRACT

A mordenite framework inverted (MFI) type zeolite membrane was produced on inexpensive tubular ceramic substrate through hydrothermal synthesis and applied for the removal of chromium from synthetic wastewater. The fabricated ceramic substrate and membrane was characterized by diverse standard techniques such as X-ray diffraction, field emission scanning electron microscope, porosity, water permeability and pore size measurements. The porosity of the ceramic substrate (53%) was reduced by the deposition of MFI (51%) zeolite layer. The pore size and water permeability of the membrane was evaluated as 0.272 μm and 4.43×10^{-7} m^3/m^2s.kPa, respectively, which are lower than that of the substrate pore size (0.309 μm) and water permeability (5.93×10^{-7} m^3/m^2s.kPa) values. To identify the effectiveness of the prepared membrane, the applied pressure of the filtration process and initial chromium concentration and cross flow rate were varied to study their influence on the permeate flux and percentage of removal. The maximum removal of chromium achieved was 78% under an applied pressure of 345 kPa and an initial feed concentration of 1,000 ppm. Finally, the efficiency of the membrane for chromium removal was assessed with other membranes reported in the literature.

Key words | chromium removal, hydrothermal treatment, MFI, zeolite membrane

R. Vinoth Kumar
G. Pugazhenthi (corresponding author)
Department of Chemical Engineering,
Indian Institute of Technology Guwahati,
Guwahati 781039,
Assam,
India
E-mail: *pugal@iitg.ernet.in*

INTRODUCTION

In recent years, environmental concerns have been increasing, particularly on the subject of heavy metals' existence in water. Heavy metals, such as chromium, lead, cadmium, mercury, nickel, copper and zinc, are, unlike organic contaminants, non-biodegradable and lead to accumulation in the human body, which causes health hazards due to their toxicity. Among these, chromium is a widespread pollutant in surface water and presents principally either in trivalent or hexavalent oxidation states. Hexavalent chromium is 10–100 times more toxic and difficult to remove from water than trivalent chromium. Moreover, it is carcinogenic to humans and causes considerable hazards to the environment (Shpiner *et al.* 2009; Kim *et al.* 2015). Therefore, the World Health Organization (WHO) set 0.05 mg L^{-1} as the highest acceptable limit for chromium in drinking water (Mandal *et al.* 2015). A variety of techniques have been established to treat chromium, including chemical precipitation (Gheju & Balcu 2011), liquid–liquid extraction (Sacmaci & Kartal 2001), chemical/electrochemical reduction (Dhaz *et al.* 2012), ion-exchange (Rengaraj *et al.* 2001), solvent extraction (Luo *et al.* 2013), adsorption (Selvi *et al.* 2001), coagulation/flocculation (Amuda *et al.* 2006), dialysis (Koseoglu *et al.* 2010) and reverse osmosis (Rad *et al.* 2009). Most of these methods have disadvantages, such as the need for pretreatment, usage of additional costly chemicals, longer operation period, etc. Moreover, these techniques are expensive and the final metal recovery requires further treatment, which causes difficulties in the

doi: 10.2166/wrd.2016.096

process and is also considered to contaminate the process itself (Canizares *et al.* 2002).

Membrane technology is the most prominent and alternative emerging process, particularly for the removal of heavy metals. This process is more economical than that of conventional/alternative techniques and requires much less land area than competing technology (Chougui *et al.* 2014). In addition, the level of efficiency is far greater than conventional treatment processes, and it allows for a high level of automation to potentially save on labor costs (Roberts *et al.* 2008). In membrane technology, ceramic membranes are extremely adaptable. They can be operated at higher temperature ranges, and many ceramic membranes are very stable at above 1,000 °C. In addition, ceramic membranes are highly stable to chemical attacks due to an extensive variety of materials utilized in preparation, which resist corrosive liquids and gases, even at higher temperatures. In the various harsh operational environments discussed above, polymeric membranes will not perform well, or will not survive at all. To reduce high transmembrane pressures and achieve higher flux than ultrafiltration, the microfiltration technique is preferable to further lower the treatment cost. Also, the ceramic membrane is prepared with a composite arrangement using an active top layer that will determine its separation efficiency. This active layer is formed using inorganic oxide materials through dip-coating, the sol-gel technique and hydrothermal treatment. In general, the active layers are fabricated using inorganic oxides such as alumina, zeolites, zirconia, titania, etc. Among these, zeolites provide well-defined pore structures, better chemical and thermal stability and exhibit excellent applications in various separation processes. In addition, zeolites possess molecular dimension channels and distinct cavities, which are uniform in size, this results in narrow pore size dispersion within the active top layer (Kumar *et al.* 2015a). Therefore, the use of a thin film of zeolite offers specific interest to obtain high selectivity in membrane separation processes.

Several researchers have reported that the separation of solutes by ultrafiltration (UF) and microfiltration (MF) is not only based on the pore size, but also depends on other factors such as the surface charge of the membrane and electrostatic interactions between the membrane and charged solutes (Monash *et al.* 2010; Kumar *et al.* 2015b). This means that the interaction between membrane and metal ions can significantly affect the performance of the UF/MF membranes. For the UF/MF of ions, the rejection is based on the chemical nature of the membrane, the physico-chemical properties of the solute and, importantly, the electrostatic interactions between membrane and ions. The retention of ions takes place due to the electrostatic interaction between the surface charge of the pores and ion molecules, and is not based on the pore size of the membrane. Nano-scale inorganic oxide materials (zeolites, ZrO_2, TiO_2/Al_2O_3, Al_2O_3 and SiO_2) were used to create the charge on the surface of the membranes (Kocherginsky *et al.* 2003; Shukla & Kumar 2005; Chang *et al.* 2014; Majhi *et al.* 2014). Among these, zeolites are crystalline aluminosilicate inorganic materials with unique intrinsic properties including superior ion-exchange ability, which form the basis for their traditional applications in the separation of small molecules. These charged membranes enable good separation efficiency, even utilizing a realistically larger range of pore size membranes. Here, the Donnan potential is produced at the interface between the UF/MF membrane and solution to maintain an electrochemical equilibrium, which facilitates the repulsion of co-ions (same charge as the membrane) by the membrane; accordingly, the separation of ions takes place with a zeolite membrane.

Recently, numerous investigations have been carried out to discover the potential of charged UF and MF membranes for the removal of chromium. Covarrubias *et al.* (2008) synthesized the FAU zeolite membrane using a secondary growth technique on an alumina support and obtained a maximum rejection of 95% for Cr(III). Doke & Yadav (2014) produced a titania MF membrane using nanocrystalline titania by the sol-gel technique, and obtained 99% removal of chromium from aqueous solution. Tang *et al.* (2012) prepared the magnetite membrane by the sol-gel technique using porous stainless steel as a support. The prepared membrane effectively removed 92.5% of chromium presented in the aqueous medium. Shukla & Kumar (2007) prepared the analcime-O zeolite composite membrane via a hydrothermal method for the separation of chromic acid solution, and attained about 50% chromium rejection using the unmodified zeolite membrane. They reported that the charged membrane can separate the acid chromate ions, even those having a bigger pore size. Tijani *et al.* (2013) investigated the preparation of NaA zeolite membranes by hydrothermal treatment at various temperatures, applied for removal of hexavalent chromium.

They strongly suggested that the zeolite membrane could be particularly useful for the separation of heavy metals. The above studies indicate that chromium removal can be attained by utilizing charged membranes, even with a bigger pore size.

It is noteworthy to point out that many of the researchers have used α-alumina as a support material to fabricate the zeolite membranes (Liu *et al.* 2007; Covarrubias *et al.* 2008; Wu *et al.* 2008; Huang *et al.* 2012). The cost of α-alumina support is very expensive (approximately $500/m^2) and also requires a higher sintering temperature (>1,200 °C) for the fabrication. Therefore, the current tendency of research is directed at utilizing alternative low cost ceramic support for making zeolite membranes to reduce the cost of the membrane. With this understanding, we prepared the mordenite framework inverted (MFI) zeolite membrane on a low cost tubular ceramic substrate and studied its potential in an industrially and environmentally related ionic removal of toxic chromium present in the aqueous medium at various operating conditions.

EXPERIMENTAL

MFI zeolite membrane preparation

The comprehensive procedure adopted for the fabrication of the MFI zeolite membrane is presented in Figure 1. The methodology followed for the fabrication of the MFI zeolite membrane on inexpensive tubular ceramic substrate and its characteristics are extensively presented in our earlier published work (Kumar *et al.* 2015b). Firstly, the tubular substrate was fabricated using cheaper natural clays with the composition of ball clay (18 wt%), feldspar (6 wt%), kaolin (15 wt%), pyrophyllite (15 wt%), quartz (28 wt%) and calcium carbonate (18 wt%). The clay mixtures were well mixed with Millipore water obtained from Milli-Q system to create a paste for the extruding tube. The paste was fed into the extrusion cylinder and extruded with the dimensions of 100 mm length, and an exterior and interior diameter of 11.5 mm and 5.5 mm, respectively. The obtained tube was air-dried for 12 h under atmospheric conditions. The ceramic tube was then dried at 100 °C for 12 h and 200 °C for 12 h in a hot air oven. Afterwards, the tube was sintered at 950 °C for 6 h in a box furnace. The sintered ceramic substrate was washed and dried at 100 °C for 6 h prior to hydrothermal coating.

Secondly, the MFI zeolite membrane was fabricated by hydrothermal technique with a gel composition of $100SiO_2{:}5(TPA)_2O{:}5.3Na_2O{:}1420H_2O$ (Wegner *et al.* 1999). This suspension, along with the above elaborated ceramic substrate, was subjected to hydrothermal treatment at 185 °C for 4 h in an autoclave reactor. After hydrothermal treatment, the membrane was calcined at 400 °C for 5 h at a heating rate of 0.5 °C/min to remove the organic template from the zeolite channels.

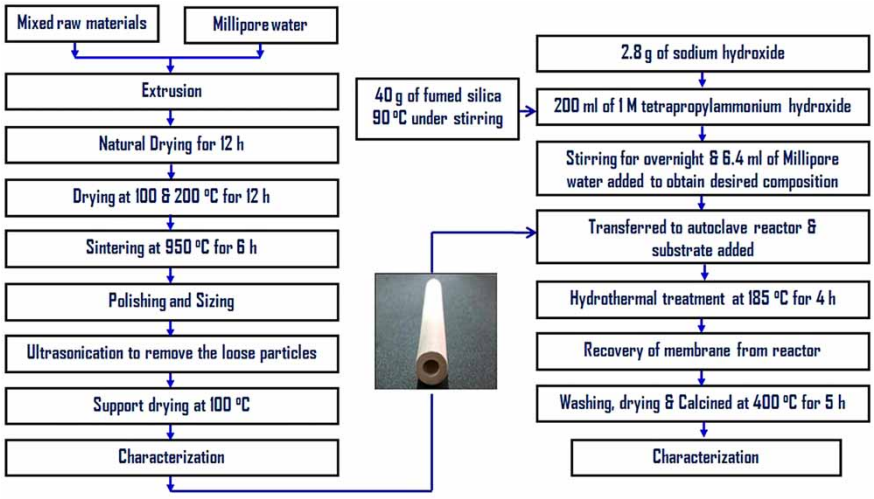

Figure 1 | Preparation of MFI zeolite membrane.

Characterization methods

The X-ray diffraction (XRD) patterns of the utilized raw materials for fabrication of the ceramic substrate and synthesized MFI zeolites were recorded on a D8 ADVANCE X-ray diffractometer in the 2θ range of 2–90 ° at a scanning rate of 0.05 °/s. Membrane morphology, including the distribution of zeolites as well as a cross-sectional view of the membrane, was observed by a field emission scanning electron microscope (FESEM, JEOL JSM-5600LV). The samples were coated with a thin layer of gold before analysis. The porosity of the membrane was measured by Archimedes principle using the below expression (Kumar *et al.* 2015b):

$$\text{Porosity}\% = \frac{W_{wet} - W_{dry}}{\rho_{water} \times V_{membrane}} \times 100 \quad (1)$$

where W_{wet}, W_{dry} are the wet and dry weights of the membrane (dried at 120 °C for 3 h), respectively. $V_{membrane}$ is the total volume of the membrane and ρ_{water} is the density of the water. In order to estimate the wet weight of the membrane, the membrane was soaked in water for 24 h. Then, the wet weight was measured after wiping all the water from the membrane surface with tissue paper. Five measurements were conducted for each sample and the average value was reported. The water permeability and pore size of the membrane was calculated by various methods, which are extensively presented in our earlier published work (Kumar *et al.* 2015b).

Water flux and chromium removal tests

The water flux of the membrane was obtained at diverse applied pressures (69–345 kPa) using the laboratory-scale cross-flow MF test unit (see Figure 2).

The water flux was calculated using the following equation:

$$J_w[flux] = \frac{Q\ [\text{volume of water permeated, } m^3]}{A\ [\text{area, } m^2] \times t\ [\text{time, s}]} \quad (2)$$

The chromium removal experiments were conducted using the same MF set up illustrated in Figure 2. The analytical grade chromium (VI) oxide (Merck (I) Ltd, Mumbai) was utilized for filtration tests. The aqueous solution of chromium was made with Millipore water and its concentration was calculated by means of conductivity (Eutech Instruments CON 2700). The filtration tests were carried out at different process conditions, such as applied pressure (69–345 kPa), initial feed concentration (250–3,000 ppm) and cross flow rate (5.55 ×

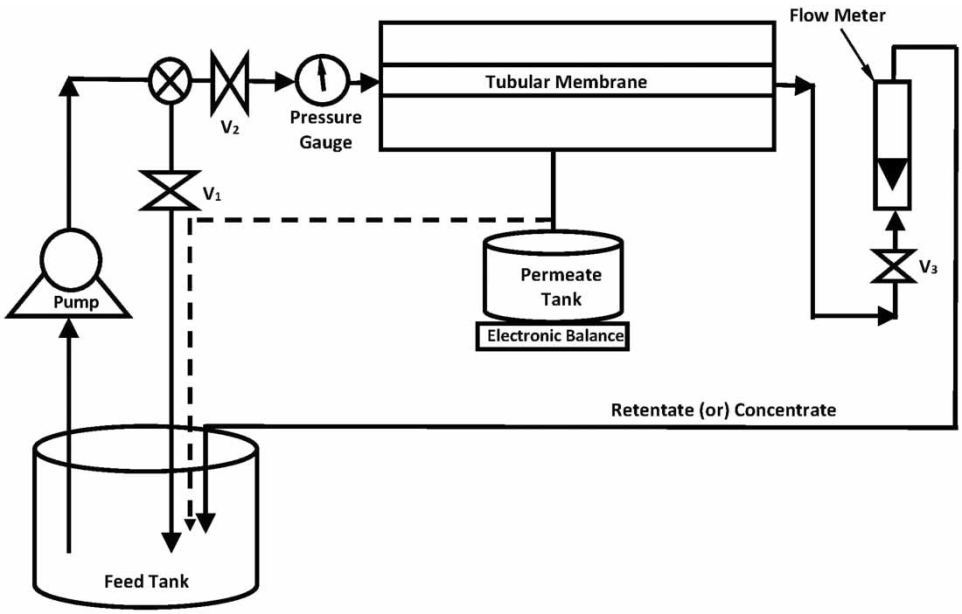

Figure 2 | Schematic of experimental setup (V_1-by-pass valve, V_2-inlet valve, V_3-retentate valve).

$10^{-7}-1.66\times10^{-6}$ m^3/s) for a period of 1 h. In order to avoid the contribution of surface adsorption of chromate ions, the first ~50 mL of permeate solution was thrown away and the subsequent permeated solution through the membrane was considered to calculate the percentage removal of chromium at each condition. The membrane was thoroughly rinsed by passing Millipore water for 1 h at a higher pressure after every MF run.

The percentage of chromium removal was calculated using the following equation:

$$R\ [\text{rejection, \%}] = 1 - \frac{c_p\ [\text{concentration in permeate}]}{c_f\ [\text{concentration in feed}]}\times 100 \quad (3)$$

RESULTS AND DISCUSSION

Characterization

All the raw materials used for fabrication of the ceramic substrate were examined using XRD and the obtained patterns match well with the Standard Joint Committee on Powder Diffraction Standards (JCPDS) files. The XRD patterns of the raw materials are presented in Figure 3. The XRD peaks of the kaolin are in good agreement with the reflections of standard JCPDS card number 14–164 and the other additional reflections also match with the JCPDS card number 10–446. This indicates that kaolin also contains dickite, which is the same composition as kaolinite with different a crystal structure (Castellano *et al.* 2010). The main crystalline phases observed in the ball clay correspond to kaolin ($2\theta = 12.25$ and 24.85°) and quartz. The 2θ reflections ($2\theta = 20.85$ and 26.65°) of quartz match well with the JCPDS card number 46–1045, which corresponds to the pure quartz phase (González *et al.* 2007). Similarly, the XRD profiles of pyrophyllite and feldspar are in excellent agreement with the standard JCPDS card numbers 12–203 and 09–456, respectively (Sugiyama *et al.* 1993).

The synthesized MFI zeolite was characterized to substantiate its pureness by the XRD profile as presented in Figure 4. The XRD pattern exhibits high crystallinity, and the acquired profile is in good agreement with profiles of MFI zeolites reported by Wegner *et al.* (1999). The characteristic peaks appeared at 2θ value of 8 and 23.5 with some other bearing peaks, indicating the existence of zeolite with pure phase.

Figure 5 shows the FESEM morphologies of the ceramic substrate (Figure 5(a) and (b)) and zeolite membrane (Figure 5(c) and (d)) at the same magnifications after the hydrothermal coating of the MFI zeolites. It can be clearly seen that the synthesized MFI zeolites are homogeneously dispersed on the membrane surfaces. In the zeolite deposition process, the layer of MFI zeolite crystals completely covers the ceramic substrate. The overall surface morphological analysis shows that the cracks do not appear on the membrane surfaces. Figure 5(e) shows MFI zeolite particles and Figure 5(f) illustrates the cross-sectional image of the MFI zeolite membrane. These figures evidently prove that the pores of the ceramic substrate are blocked by the zeolite particles.

The average porosity is measured as 53% for the ceramic substrate and 51% for the zeolite membrane according to methods reported elsewhere (Kumar *et al.* 2015b). The water flux obtained for the ceramic substrate and zeolite membrane is presented in Figure 6. As expected, water flux increases linearly with an increase in the applied pressure and follows Darcy's law. Figure 6(b) depicts the pure water flux of the ceramic substrate along with the zeolite membrane as a function of applied pressure. It is evident from the figure that the water flux of the zeolite membrane is lower than the ceramic substrate. It is accredited by the reduction in pore radius on hydrothermal treatment. The water permeability is calculated as 5.93×10^{-7} m^3/m^{2}s kPa for the ceramic substrate and 4.43×10^{-7} m^3/m^{2}s kPa for the zeolite membrane from the slope of the water flux versus pressure across the membrane (from Figure 6(b)). The average hydraulic pore size is determined using the Hagen Poiseuille expression by assuming pores are cylindrical in shape (Kumar *et al.* 2015b):

$$J_w = \frac{\varepsilon r^2 \Delta P}{8\mu\tau l} = L_h \Delta P \quad (4)$$

where ε is the porosity of the membrane, r is the pore radius of the membrane, l is the pore length, τ is the tortuosity factor, μ is the viscosity of water, L_h is water permeability and ΔP is the applied pressure. The average hydraulic pore

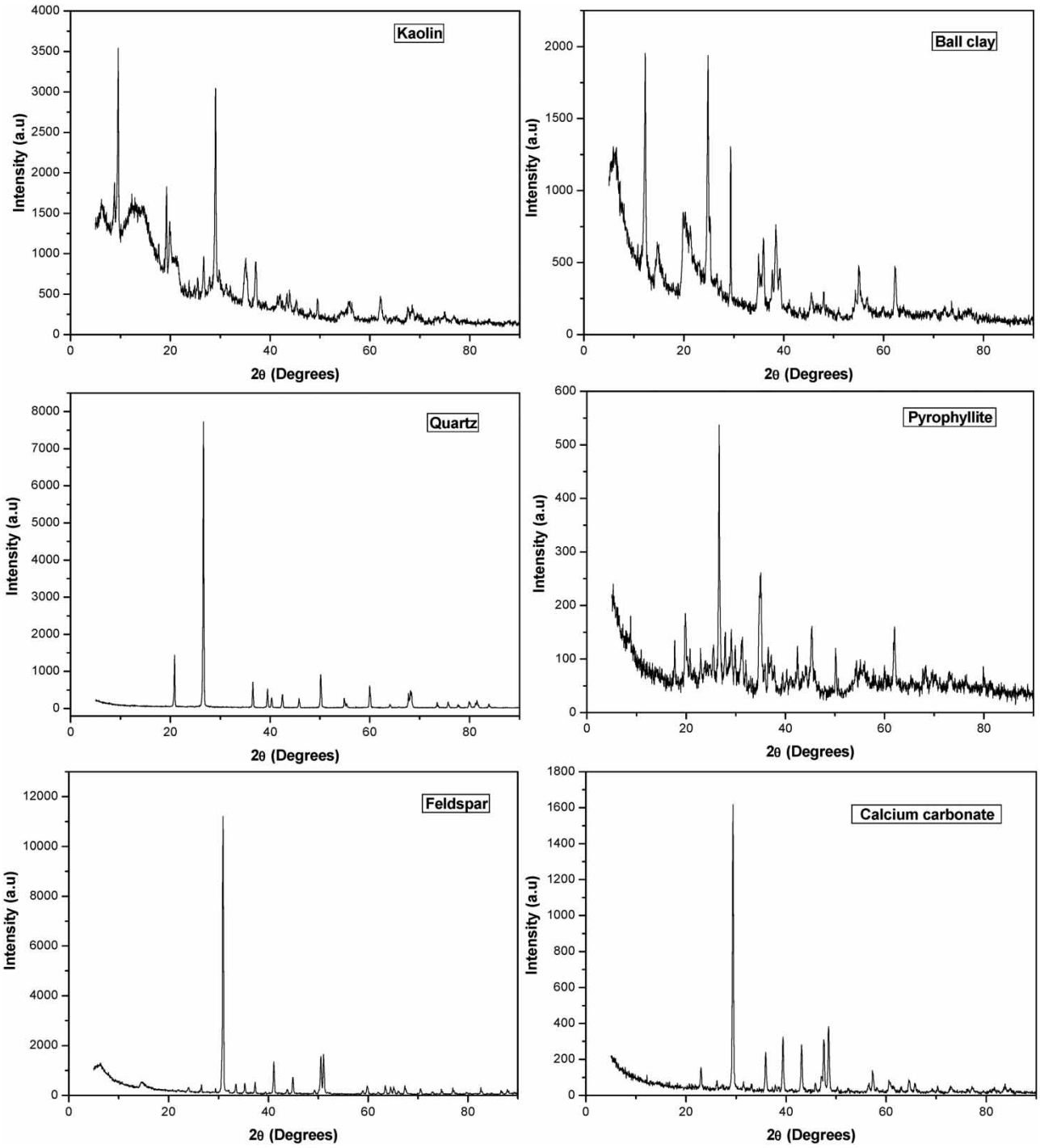

Figure 3 | XRD patterns of the raw materials used for the preparation of the substrate.

diameter of the ceramic substrate is estimated to be 0.309 μm, whereas for the zeolite membrane it is found to be 0.272 μm, which represents the pore size of the top separating layer. It is worth mentioning that the hydrothermal coating of zeolite on the ceramic substrate reduced the porosity, permeability and pore size values.

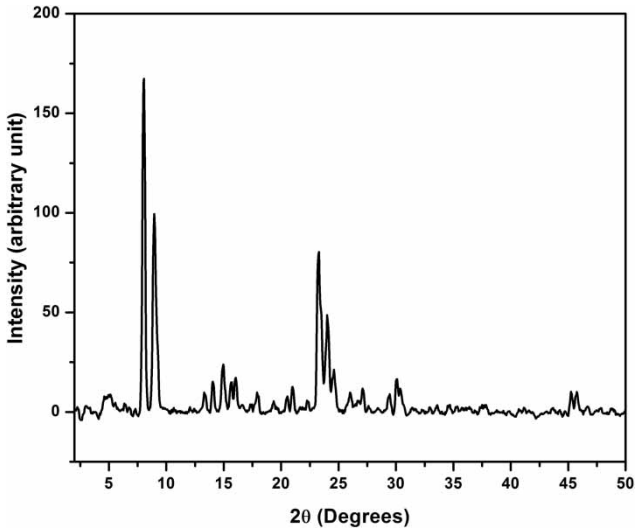

Figure 4 | XRD analysis of MFI zeolite.

Performance of MFI zeolite membrane in removal of chromium

To identify the effectiveness of the prepared MFI zeolite membrane on the permeate flux and for chromium removal, variables such as applied pressure, initial chromium concentration and cross flow rates were varied and the effects of the same on the membrane were studied.

Effect of applied pressure

Figure 7(a) shows the permeate flux with time for the MFI zeolite membrane at various applied pressures. The permeate flux is almost constant for the entire operation period as displayed in Figure 7(a). This is probably owing to the insignificant contribution of adsorption on the membrane surface. On the other hand, the chromium flux is marginally less than that of the water flux of the membrane. This typical trend is obtained owing to the generation of osmotic pressure by the retained ions, which leads to a decrease in the effectual pressure on the membrane surface. Figure 7(b) shows the percentage removal of chromium at different applied pressures. The removal of chromium gradually augments with the filtration time, which is possibly due to the development of concentration polarization, until the steady state is reached with time on the surface of the membrane. The percentage of chromium removal increases with an increase in the applied pressure. The formation of the concentration polarization effect does not occur in the initial period of operation and at low applied pressure. Conversely, it develops with increasing time owing to the retention of ions within the membrane pores. When the applied pressure increases, the convective transport becomes more significant than the diffusive transport. As a result, the percentage removal of chromium enhances with increasing pressure due to the dilution effect, as the higher transport of solvent flux would result in a dilution of the permeate. Therefore, the higher applied pressure enables a higher removal of chromium (Gherasim & Mikulasek 2014). The maximum removal of chromium (78%) is achieved under the applied pressure of 345 kPa.

It is worth mentioning that the surface charge of the membrane is a key factor for the influential removal efficacy of the membrane while dealing with an ionic solution. Even if the pore size of the membrane is relatively larger than the size of the charged solute, the removal of solute by zeolite membranes can take place due to electrostatic interactions between the charged membrane and solute (Monash *et al.* 2010; Kumar *et al.* 2015b). The surface charge of the membrane pores depends on the pH of the contact solution, and it can be either positive or negative. In order to find out the surface charge of the MFI membrane, the zeta potential of the MFI particles (calcined) was measured using an electrophoretic light scattering method in Delsa Nano C (Beckman coulter) by keeping the powders in water suspension at different pH. The surface charge of the MFI powder was altered by the addition of HCl to make a lower pH, and for a higher pH, NaOH solution was added. At a lower pH, the surface charge of the MFI powder becomes positive due to a larger quantity of H^+ ions, whereas at higher pH, negative hydroxyl (OH^-) ions increase owing to the addition of NaOH (see Figure 8). The zeta potential value of MFI is around +11.5 mV at an acidic pH (pH = 2) and at pH 12, it is approximately −63 mV (Figure 8). It is clear from these data that the electrostatic interactions play a major role in the surface activity of MFI. In this study, the iso-electric point (IEP) of the MFI powder is found to be 4, which is in good agreement with the IEP value reported by Kosmulski (2009) for MFI zeolite.

Since the IEP of the MFI is 4, the membrane is positively charged at a pH less than 4, and the membrane is negatively

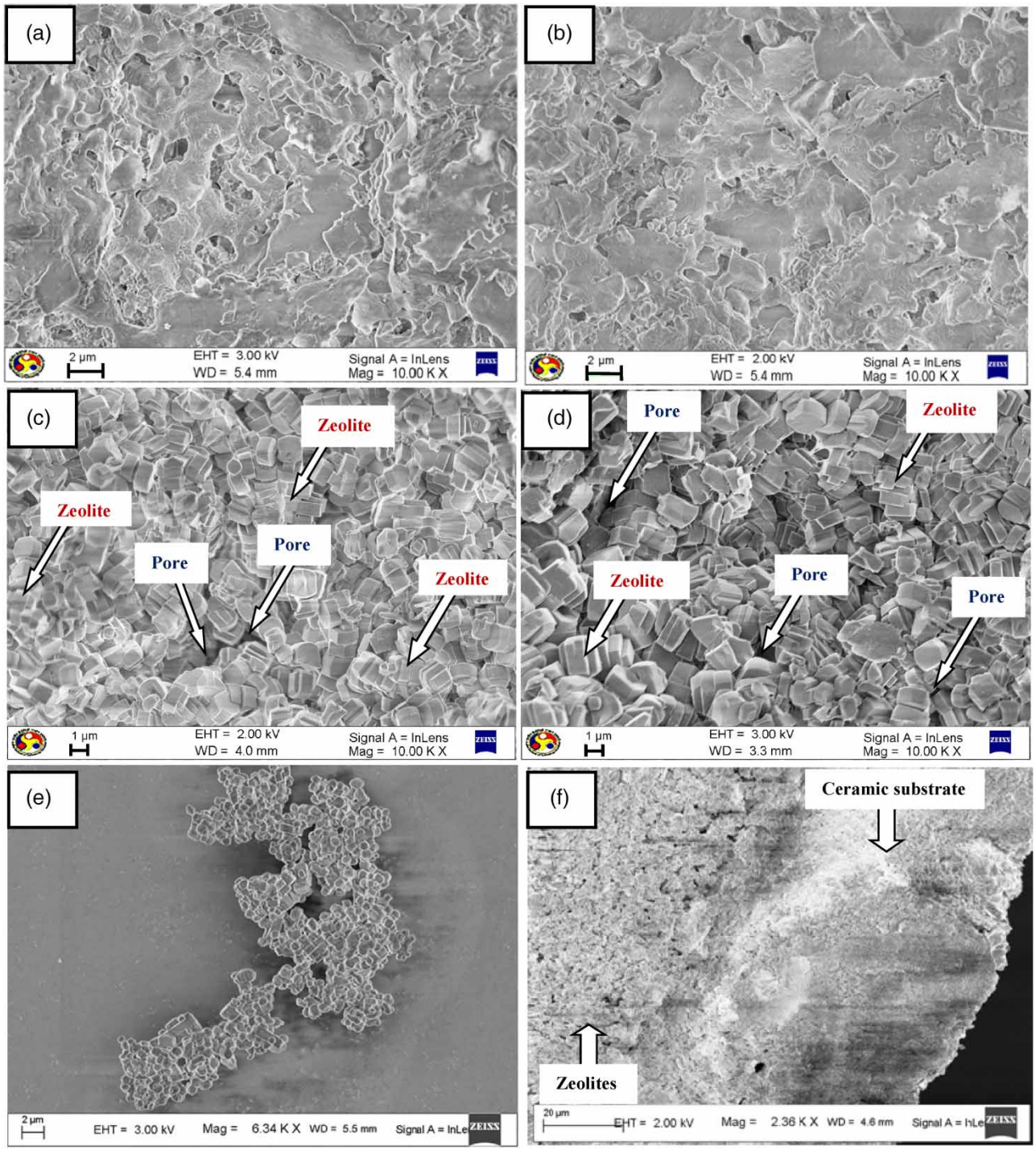

Figure 5 | (a) and (b) FESEM images of the inner and outer surfaces of the substrate; (c) and (d) inner and outer surfaces of the MFI zeolite membrane; (e) MFI zeolite particles; and (f) cross-sectional view of the MFI zeolite membrane.

charged when the pH of the solution is greater than 4. When the charged membrane is in contact with chromic acid solution, the concentration of ions with the same charge as the membrane will be lower near the surface of the membrane than that in the solution, and the other ions, which have the opposite charge, have a higher concentration in

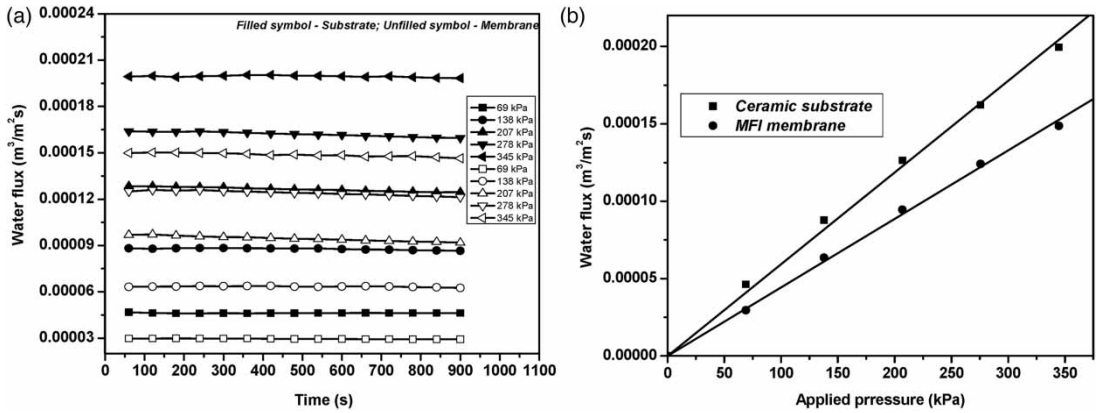

Figure 6 | (a) Water flux as a function of time for pressures and (b) water flux as a function of applied pressure for the ceramic substrate and zeolite membrane.

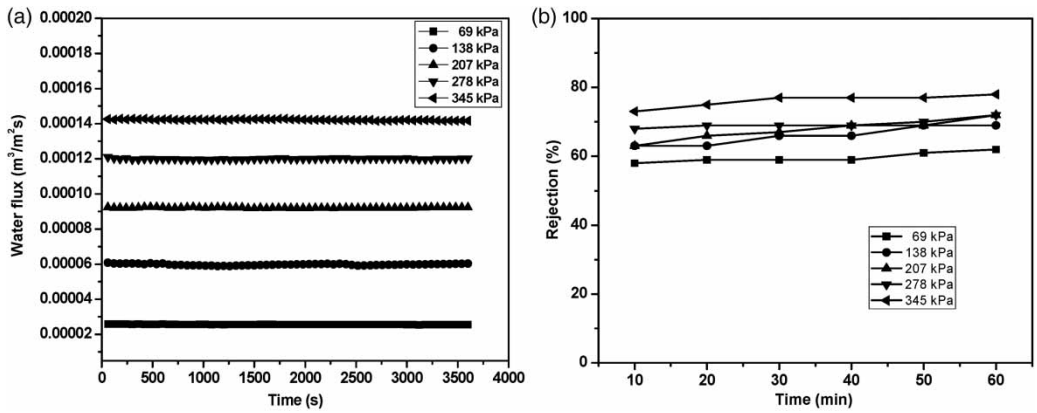

Figure 7 | Effect of applied pressure on (a) permeate flux and (b) removal (%) for the MFI membrane (applied pressure: 69–345 kPa; cross flow rate: 1.11×10^{-6} m^3/s; feed concentration: 1,000 ppm).

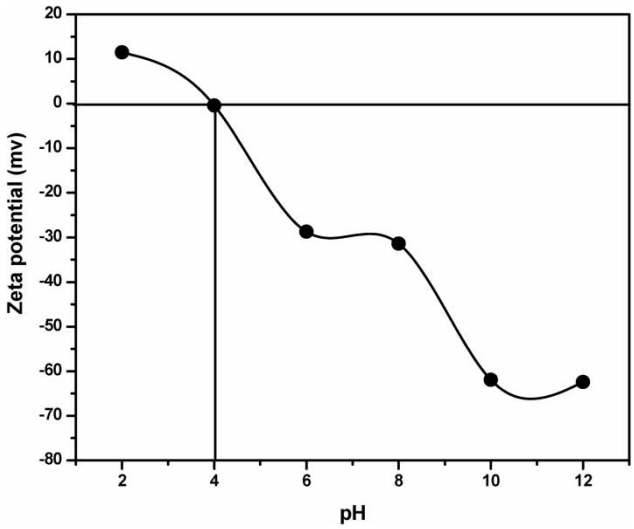

Figure 8 | Zeta potential measurement of MFI zeolites at various pH.

the membrane than in the solution. On account of this concentration difference, a potential difference is generated at the interface between the membrane and the solution to maintain electrochemical equilibrium between the solution and membrane. With this potential, the membrane repels the ions with the same charge as the membrane (Chung *et al.* 2005). In aqueous solution, chromium is usually present in the form of $HCrO_4^-$, $Cr_2O_7^{2-}$ and CrO_4^{2-} (Benhamou *et al.* 2013). In this study, the removal experiments were conducted at the natural pH of the chromium solution (~2.35). The chromium predominantly presents in the form of acid chromate ions ($HCrO_4^-$) along with H_3O^+ in this experimental condition (Benhamou *et al.* 2013; Basumatary *et al.* 2015). Since the membrane is positively charged at this pH condition, therefore, repulsion between the positively charged membrane and positive species (H_3O^+) will

take place. As the cation and anion cannot act autonomously, thereby $HCrO_4^-$ is also rejected to maintain the electroneutrality of the system, as shown in Figure 9 (Benhamou *et al.* 2013; Basumatary *et al.* 2015; Kumar *et al.* 2015a).

Effect of concentration

Figure 10(a) demonstrates the permeate flux with time for the MFI zeolite membrane at various feed concentrations. It is evident from the figure that there is a marginal decline in the flux when the chromium concentration gradually increases. This is probably due to the occurrence of incomplete plugging of the membrane pores. This leads to the creation of another barrier layer, which may have reduced the flux at higher concentrations of chromium. The permeate flux of chromium slightly declines with the extension of operation time. This decrement in permeate flux is probably due to the chromium ions fouling (Habibi *et al.* 2015). It is apparent that the percentage removal of chromium augments with an increment in the initial feed concentration of chromium, as displayed in Figure 10(b). This is primarily attributed to various factors such as concentration polarization, osmotic pressure and membrane fouling across the membrane surface. In the studied concentration range (500–3,000 ppm) the highest percentage removal obtained was 76% for the initial chromium concentration of 3,000 ppm.

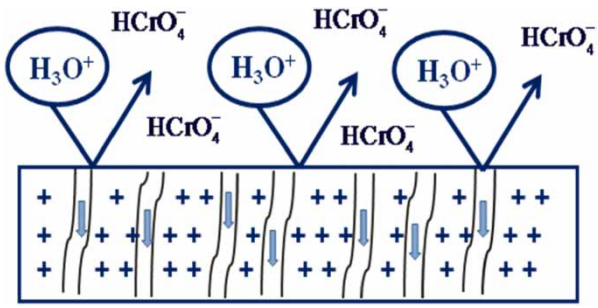

Figure 9 | Schematic representation of chromium ion repulsion.

Effect of cross flow rate

Figure 11(a) depicts the variation in permeate flux with time for MFI zeolite membrane at various feed cross flow rates. The permeate flux augments with increasing cross flow rate due to the decrement in concentration polarization at the higher cross flow rate. An increase in the cross flow rate induces shear stress across the membrane surface, thereby minimizing the chance of chromium adsorption on the membrane surface. The cross flow rate plays a substantiate role in diminishing the concentration polarization by its wiping behavior on the membrane surface. Therefore, the probability of causing resistance as well as fouling is lower, as shown in Figure 11(a). Moreover, the convective force is improved, while a decrement in concentration polarization thereby enhances the solvent flux owing to its

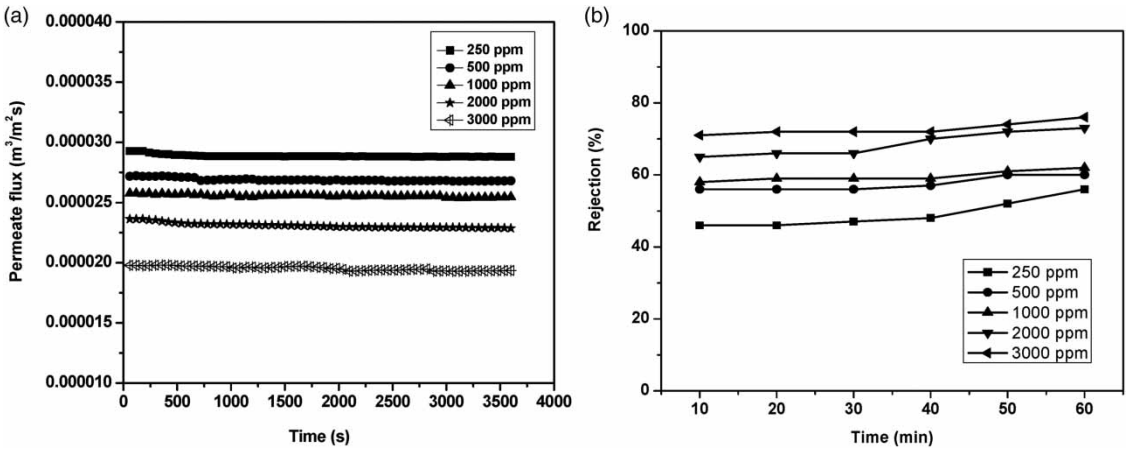

Figure 10 | Effect of initial feed concentration on (a) permeate flux and (b) removal (%) for the MFI membrane (feed concentration: 250–3,000 ppm; applied pressure: 69 kPa; cross flow rate: 1.11×10^{-6} m^3/s).

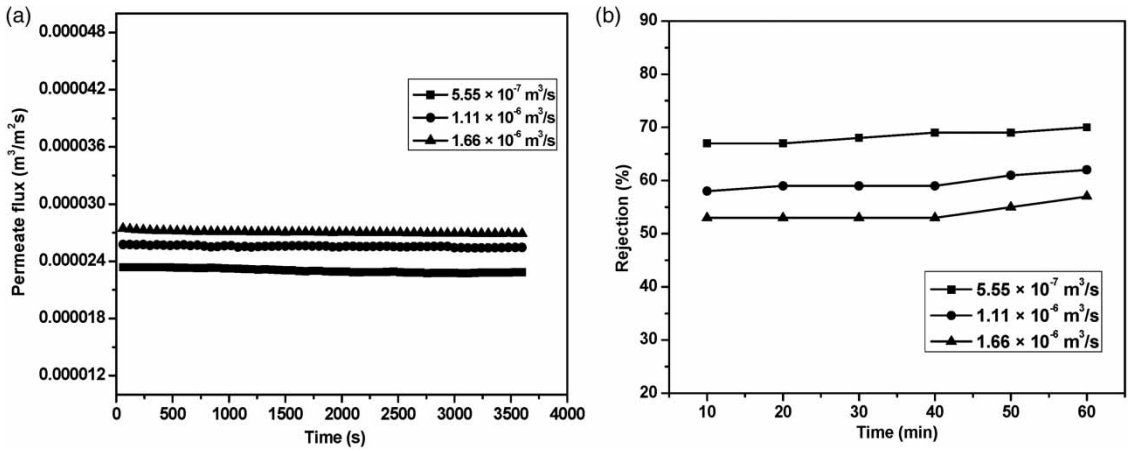

Figure 11 | Effect of cross flow rate on (a) permeate flux and (b) removal (%) for MFI membrane (cross flow rate: 5.55×10^{-7}–1.66×10^{-6} m^3/s; applied pressure: 69 kPa; feed concentration: 1,000 ppm).

uncoupling nature of the solvent and solute flux during operation. It is noticeable that the percentage removal of chromium slightly declines with an increase in cross flow rate, as depicted in Figure 11(b). This is probably attributed to the thinner boundary layer on the membrane surface at a high cross flow rate. The balance between convective transport from bulk to membrane surface and the solute's diffusive transport from membrane surface to bulk at steady state may result in a higher concentration of solute at the membrane. Therefore, the chromate ions can easily reach the permeate side and decrease the removal (Danis & Keskinler 2009). For this reason, the percentage of chromium removal decreases with a rise in the cross flow rate. In the investigated cross flow rates, the maximum removal of chromium obtained was 70% at the lower cross flow rate of 5.55×10^{-7} m^3/s.

Performance assessment of MFI membrane on chromium removal

The efficiency of the fabricated MFI zeolite membrane on chromium removal is assessed with other membranes reported in the literature (Neelakandan *et al.* 2003; Pugazhenthi *et al.* 2005; Shukla & Kumar 2007; Sachdeva & Kumar 2008; Ren *et al.* 2010; Vinodhini & Sudha 2016). From the assessment survey (Table 1), the highest removal of 78% with a permeate flux of 1.42×10^{-4} m^3/m^2s achieved in this work is better than that of other membranes. Even though some of the membranes showed a higher percentage removal of chromium in comparison with this work, the flux (1.42×10^{-4} m^3/m^2s) of the present study is 1–6 orders higher when compared with other membranes (see Table 1), and also the membrane displays a reasonable removal percentage (78%). Thus, the prepared MFI zeolite

Table 1 | Potential assessment of the prepared membrane with other membranes on chromium(VI) removal

Membrane material	Pore size	Feed concentration (ppm)	Solute permeability (m^3/m^2s)	Rejection (%)	References
PMMA-EGDM	8.5 kDa	1,000	5.96×10^{-10}	68	Neelakandan *et al.* (2003)
Zeolite-clay membrane	30 nm	1,000	2.73×10^{-6}	66	Shukla & Kumar (2007)
Clay-carbon	2 nm	1,000	1.46×10^{-8}	96	Pugazhenthi *et al.* (2005)
Styrene acrylonitrile	55 nm	1,000	2.38×10^{-6}	90	Sachdeva & Kumar (2008)
CA-NCS-PEG	–	1,055	7.03×10^{-7}	95	Vinodhini & Sudha (2016)
PMIA membrane	32 nm	130	2.07×10^{-5}	90	Ren *et al.* (2010)
MFI-type zeolite membrane	0.272 μm	1,000	1.42×10^{-4}	78	This study

membrane proved to be better in comparison with other membranes for chromium removal.

CONCLUSIONS

An MFI-type zeolite membrane was successfully produced on inexpensive tubular ceramic substrate through a hydrothermal synthesis method. The ceramic substrate was layered with homogeneous dispersion of MFI zeolite crystals to form a uniform MFI zeolite membrane. The efficiency of the prepared zeolite membrane was tested by the removal of chromium present in the aqueous medium. The highest rejection of 78% was achieved with a permeate flux of 1.42×10^{-4} m^3/m^2s. The performance comparison analysis clearly indicated that the prepared membrane has better potential in the removal of chromium while offering better flux.

ACKNOWLEDGEMENTS

The authors would like to thank the Central Instruments Facility at IIT Guwahati for helping us to perform FESEM analysis.

REFERENCES

Amuda, O. S., Amoo, I. A., Ipinmoroti, K. O. & Ajayi, O. O. 2006 Coagulation/flocculation process in the removal of trace metals present in industrial wastewater. *J. Appl. Sci. Environ. Mgt* **10**, 159–162.

Basumatary, A. K., Kumar, R. V., Ghoshal, A. K. & Pugazhenthi, G. 2015 Synthesis and characterization of MCM-41-ceramic composite membrane for the separation of chromic acid from aqueous solution. *J. Memb. Sci.* **475**, 521–532.

Benhamou, A., Basly, J. P., Baudu, M., Derriche, Z. & Hamacha, R. 2013 Amino-functionalized MCM-41 and MCM-48 for the removal of chromate and arsenate. *J. Colloid Interface Sci.* **404**, 135–139.

Canizares, P., Perez, A. & Camarillo, R. 2002 Recovery of heavy metal by means of ultrafiltration with water-soluble polymers: calculation of design parameters. *Desalination* **144**, 279–285.

Castellano, M., Turturro, A., Riani, P., Montanari, T., Finocchio, E. & Ramis, G. 2010 Bulk and surface properties of commercial kaolins. *Appl. Clay Sci.* **48**, 446–454.

Chang, Q., Zhou, J., Wang, Y., Liang, J., Zhang, X., Cerneaux, S., Wang, X., Zhu, Z. & Dong, Y. 2014 Application of ceramic microfiltration membrane modified by nano-TiO_2 coating in separation of a stable oil-in-water emulsion. *J. Memb. Sci.* **456**, 128–133.

Chougui, A., Zaiter, K., Belouatek, A. & Asli, B. 2014 Heavy metals and color retention by a synthesized inorganic membrane. *Arabian J. Chem.* **7**, 817–822.

Chung, C. V., Buu, N. Q. & Chau, N. H. 2005 Influence of surface charge and solution pH on the performance characteristics of a nanofiltration membrane. *Sci. Technol. Adv. Mater.* **6**, 246–250.

Covarrubias, C., Garcia, R., Arriagada, R., Yanez, J., Ramanan, H., Lai, Z. & Tsapatsis, M. 2008 Removal of trivalent chromium contaminant from aqueous media using FAU-type zeolite membranes. *J. Memb. Sci.* **312**, 163–173.

Danis, U. & Keskinler, B. 2009 Chromate removal from wastewater using micellar enhanced cross flow filtration: effect of transmembrane pressure and cross flow velocity. *Desalination* **249**, 1356–1364.

Dhaz, C. E. B., Lugo, V. L. & Bilyeu, B. 2012 A review of chemical, electrochemical and biological methods for aqueous Cr(VI) reduction. *J. Hazard. Mater.* **223–224**, 1–12.

Doke, S. M. & Yadav, G. D. 2014 Process efficacy and novelty of titania membrane prepared by polymeric sol-gel method in removal of chromium(VI) by surfactant enhanced microfiltration. *Chem. Eng. J.* **255**, 483–491.

Gheju, M. & Balcu, I. 2011 Removal of chromium from Cr(VI) polluted wastewaters by reduction with scrap iron and subsequent precipitation of resulted cations. *J. Hazard. Mater.* **196**, 131–138.

Gherasim, C. V. & Mikulasek, P. 2014 Influence of operating variables on the removal of heavy metal ions from aqueous solutions by nano filtration. *Desalination* **343**, 67–74.

González, J., Carreras, A. & Ruiz, M. D. C. 2007 Phase transformations in clays and kaolins produced by thermal treatment in chlorine and air atmospheres. *Latin Am. Appl. Res.* **37**, 133–139.

Habibi, S., Nematollahzadeh, A. & Mousavi, S. A. 2015 Nano-scale modification of polysulfone membrane matrix and the surface for the separation of chromium ions from water. *Chem. Eng. J.* **267**, 306–316.

Huang, A., Wang, N. & Caro, J. 2012 Seeding-free synthesis of dense zeolite FAU membranes on 3-aminopropltriethoxysilane-fucntionalized alumina supports. *J. Memb. Sci.* **389**, 272–279.

Kim, M. K., Sundaram, K. S., Iyengar, G. A. & Lee, K. P. 2015 A novel chitosan functional gel included with multiwall carbon nanotube and substituted polyaniline as adsorbent for efficient removal of chromium ion. *Chem. Eng. J.* **267**, 51–64.

Kocherginsky, N. M., Tan, C. L. & Lu, W. F. 2003 Demulsification of water-in-oil emulsion via filtration through a hydrophilic polymer membrane. *J. Memb. Sci.* **220**, 117–128.

Koseoglu, T. S., Kir, E., Ozkorucuklu, S. P. & Karamizrak, E. 2010 Preparation and characterization of P2Fan/PVDF composite cation-exchanger membranes for the removal of Cr(III) and Cu(II) by Donnan dialysis. *React. Funct. Polym.* **11**, 900–907.

Kosmulski, M. 2009 pH-dependent surface charging and points of zero charge. IV. Update and new approach. *J. Colloid Interface Sci.* **337**, 439–448.

Kumar, R. V., Basumatary, A. K., Ghoshal, A. K. & Pugazhenthi, G. 2015a Performance assessment of an analcime-C zeolite-ceramic composite membrane by removal of Cr(VI) from aqueous solution. *RSC Adv.* **5**, 6246–6254.

Kumar, R. V., Moorthy, I. G. & Pugazhenthi, G. 2015b Modelling and optimization of critical parameters by hybrid RSM-GA for the separation of BSA using tubular configured MFI-type zeolite microfiltration membrane. *RSC Adv.* **5**, 87645–87659.

Liu, C., Wang, L., Ren, W., Rong, Z., Wang, X. & Wang, J. 2007 Synthesis and characterization of a mesoporous silica (MCM-48) membrane on a large-pore α-Al_2O_3 ceramic tube. *Micropor. Mesopor. Mater.* **106**, 35–39.

Luo, J. H., Li, J., Qi, Y. B. & Cao, Y. Q. 2013 Study on the removal of chromium(III) by solvent extraction. *Desalin. Water. Treat.* **51**, 2130–2134.

Majhi, A., Monash, P. & Pugazhenthi, G. 2014 Fabrication and characterization of γ-Al_2O_3-clay composite membrane ultrafiltration membrane for the separation of electrolytes from its aqueous solution. *J. Memb. Sci.* **340**, 181–191.

Mandal, S., Mahapatra, S. S. & Patel, R. K. 2015 Neuro fuzzy approach for arsenic(III) and chromium(VI) removal from water. *J. Wat. Proc. Eng.* **5**, 58–75.

Monash, P., Majhi, A. & Pugazhenthi, G. 2010 Separation of bovine serum albumin (BSA) using γ-Al_2O_3–clay composite ultrafiltration membrane. *J. Chem. Technol. Biotechnol.* **85**, 545–554.

Neelakandan, C., Pugazhenthi, G. & Kumar, A. 2003 Preparation of NO_x modified PMMA-EGDM composite membrane for the recovery of chromium (VI). *Eur. Polym. J.* **39**, 2383–2391.

Pugazhenthi, G., Sachan, S., Kishore, N. & Kumar, A. 2005 Separation of chromium(VI) using modified ultrafiltration charged carbon membrane and its mathematical modeling. *J. Memb. Sci.* **254**, 229–239.

Rad, S. A. M., Mirbagheri, S. A. & Mohammadi, T. 2009 Using reverse osmosis membrane for chromium removal from aqueous solution. *World. Acad. Sci. Eng. Technol.* **57**, 348–352.

Ren, X., Zhao, C., Du, S., Wang, T., Luan, Z., Wang, J. & Hou, D. 2010 Fabrication of asymmetric poly (m-phenylene isophthalamide) nanofiltration membrane for chromium(VI) removal. *J. Environ. Sci.* **22** (9), 1335–1341.

Rengaraj, S., Yeon, K. H. & Moon, S. H. 2001 Removal of chromium from water and wastewater by ion exchange resins. *J. Hazard. Mater. B.* **87**, 273–287.

Roberts, D., Kubel, D., Carrie, A., Schoeder, D. & Sorensen, C. 2008 *Costs and Benefits of Complete Water Treatment Plant Automation*. 1st edn. American Water Works Association, Denver, USA.

Sachdeva, S. & Kumar, A. 2008 Synthesis and modeling of composite poly(styrene-co-acrylonitrile) membrane for the separation of chromic acid. *J. Memb. Sci.* **307**, 37–52.

Sacmaci, S. & Kartal, S. 2001 Separation and enrichment of Cr(III) and Cr(VI) in environmental samples by ion-pair solvent extraction using a β-diketone ligand. *Int. J. Environ. Anal. Chem.* **5**, 448–461.

Selvi, K., Pattabhi, S. & Kadirvelu, K. 2001 Removal of Cr(VI) from aqueous solution by adsorption onto activated carbon. *Bioresour. Technol.* **80**, 87–89.

Shpiner, R., Vathi, S. & Stuckey, D. C. 2009 Treatment of oil well 'produced water' by waste stabilization ponds: removal of heavy metals. *Water Res.* **43**, 4258–4268.

Shukla, A. & Kumar, A. 2005 Characterization of chemically modified zeolite-clay composite membranes using separation of trivalent cations. *Sep. Purif. Technol.* **41**, 83–89.

Shukla, A. & Kumar, A. 2007 Separation of Cr(VI) by zeolite-clay composite membranes modified by reaction with NOx. *Sep. Purif. Technol.* **52**, 423–429.

Sugiyama, K., Ryu, H. & Waseda, Y. 1993 Local ordering structure of meta-kaolinite and meta-dickite by the X-ray radial distribution function analysis. *J. Mater. Sci.* **28**, 2783–2788.

Tang, W., Peng, Z., Li, L., Yue, T., Wang, J., Li, Z., Li, R., Chen, J., Colvin, V. L. & Yu, W. W. 2012 Porous stainless steel supported magnetite crystalline membranes for hexavalent chromium removal from aqueous solutions. *J. Memb. Sci.* **392–393**, 150–156.

Tijani, N., Ahlafi, H., Smaihi, M. & Mansouri, A. E. 2013 Preparation and characterization of NaA zeolite membranes and its application for removal of heavy metals. *Mediterr. J. Chem.* **2**, 484–492.

Vinodhini, P. A. & Sudha, P. N. 2016 Removal of heavy metal chromium from tannery effluent using ultrafiltration membrane. *Textiles Clothing Sustain.* **2** (5), 1–15.

Wegner, K., Dong, J. & Lin, Y. S. 1999 Polycrystalline MFI zeolite membranes: xylene pervaporation and its implication on membrane microstructure. *J. Memb. Sci.* **158**, 17–27.

Wu, S., Yang, J., Lu, J., Zhou, Z., Kong, C. & Wang, W. 2008 Synthesis of thin and compact mesoporous MCM-48 membrane on vacuum-coated α-Al_2O_3 tube. *J. Memb. Sci.* **319**, 231–237.

First received 25 May 2016; accepted in revised form 3 July 2016. Available online 24 August 2016